**International Conference on Space Optics—ICSO 2014**
La Caleta, Tenerife, Canary Islands
7–10 October 2014

*Edited by Zoran Sodnik, Bruno Cugny, and Nikos Karafolas*

# *The use of a cubesat to validate technological bricks in space*

*E. Rakotonimbahy*

*S. Vives*

*K. Dohlen*

*G. Savini*

*et al.*

esa icso proceedings cnes

International Conference on Space Optics — ICSO 2014, edited by Zoran Sodnik, Nikos Karafolas,
Bruno Cugny, Proc. of SPIE Vol. 10563, 105633F · © 2014 ESA and CNES
CCC code: 0277-786X/17/$18 · doi: 10.1117/12.2304223

# THE USE OF A CUBESAT TO VALIDATE TECHNOLOGICAL BRICKS IN SPACE

E. Rakotonimbahy[1], S. Vives[1], K. Dohlen[1], G. Savini[2], V. Iafolla[3]
[1] *CNRS, LAM (Laboratoire d'Astrophysique de Marseille) UMR 7326, 13388, Marseille, France.*
[2] *Optical Science Laboratory, Physics & Astronomy Department,*
*University College London, London WC1E 6BT, UK.*
[3] *IAPS - Institute for Space Astrophysics and Planetary Sciences,*
*INAF, National Institute of Astrophysics, Rome, Italy*

## I. ABSTRACT

In the framework of the FP7 program FISICA (Far Infrared Space Interferometer Critical Assessment), we are developing a cubesat platform which will be used for the validation in space of two technological bricks relevant for FIRI.

The first brick is a high-precision accelerometer which could be used in a future space mission as fundamental element for the dynamic control loop of the interferometer.

The second brick is a miniaturized version of an imaging multi-aperture telescope. Ultimately, such an instrument could be composed of numerous space-born mirror segments flying in precise formation on baselines of hundreds or thousands of meters, providing high-resolution glimpses of distant worlds. We are proposing to build a very first space-born demonstrator of such an instrument which will fit into the limited resources of one cubesat.

In this paper, we will describe the detailed design of the cubesat hosting the two payloads.

## II. CONTEXT

Offering the advantages of low cost and rapid development, CubeSats are considered excellent platforms for space-born testing of key technologies. This is why the development of such a mission is included as part of the FISICA study, aiming to improve the Technology Readiness Level (TRL) of a future large infrared space missions, such as FIRI (Far IR Interferometer).

A cubesat is a standard of nano-satellite for space research that usually presents itself as a combination of 1, 2 or 3 satellite units (U), each of which has a volume of exactly one liter (10 cm cube), has a mass of no more than 1.33 kilograms, and typically uses commercial off the-shelf (COTS) components for its electronics. Cubesats offer the advantages to be developed in a very short time-scale with low cost and they are usually launched in 'piggyback', using excess capacity of launch vehicle.

The Far Infrared Space Interferometer Critical Assessment study (FISICA) is a research program conducted with EU funding within the FP7 framework. One of its aims is to develop a CubeSat platform for testing key space technology bricks applicable to a future FIR interferometry mission. While the critical technology brick that was selected for implementation on such a platform was an accelerometer under development by Assist in Gravitation and Instrumentation (AGI) in Rome [1], it was decided to also implement a miniature, non free-flying, demonstration of the hypertelescope concept [2].

## III. THE CUBESAT PLATFORM

A 2 Unit cubesat will be required for this mission. The following standard avionics will be on board [3]:

- ➢ NanoPower P-series for the power module, which will provide photovoltaic power conversion up to 10W with an on board 1.8 Ah lithium ion batteries, allowing up to 6 hour autonomy for the cubesat.
- ➢ Nanomind A712C for the on board computer with its high-performance 32-bit ARM7 RISC CPU and 2GB MicroSD card support for data (especially for pictures)
- ➢ Nanocom U482C for communication system, providing up to 4800 baud uplink and 9600 baud downlink for data transfer

These modules are fully compatible with the cubesat standard:

- Dimension: 96 mm x 90 mm
- Low mass

- I²C, CAN, USART interfaces available
- 104-pin cubesat kit bus connector

The Attitude Determination and Control System (ADCS) occupies 1/2U and features a 3-axis magnetometer and a sun senor, 3 electromagnets and an ADACS computer for a stand-alone, plug-and-play attitude control system for small satellites in addition to the reaction wheel for accelerometer testing [4]. It will be placed at the top of the cubesat as shown on Figure 1 (left), with the accelerometer (in green) and avionics in the left-hand unit and a rough representation of the ADCS module (in yellow) and space for the second payload in the right-hand unit. Required ADCS performances are listed in Table 1.

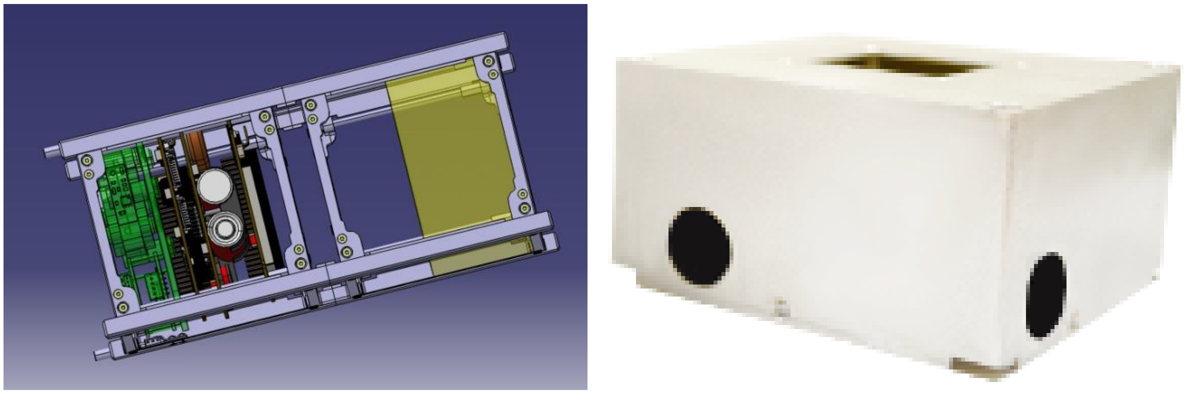

**Figure 1**: Components arrangement on left and the ADCS module on right

**Table 1 :** ADCS characteristics

| **Performance Item** | **Unit** | **Specification** |
|---|---|---|
| Dimensions | cm | 10 x 10 x 5.6 (max height) |
| Operating Temperature | deg C | -40 to 85 |
| Weight | g | 694 |
| Interface | | RS-232 (Optional I2C, CAN, SPI, USB) |
| DC Voltage | V | 5V |
| Current | A | 0.4 (Steady State) |
| Momentum Storage | mNms | 9.3 |
| Maximum Torque | mNm | 0.635 |

## IV. ACCELEROMETER

### *A. Purpose*

The use of accelerometers on board of the formation flying satellites offers the opportunity to implement control loop algorithms keeping the satellites in the appropriate positions with the necessary precision during the observation periods.

The cube-sat implementation of a single-axis version of such an accelerometer is designed to demonstrate the Technology Readiness Level (TRL) of this key elements for a Far-Infrared interferometer, i.e. the functionality of an accelerometer that can be the fundamental element to be used in a control loop of the interferometer to control its dynamic.

### *B. Main Characteristics*

In this section will be described the general aspects related to the characteristics of an accelerometer which both seems to meet the requirements for its use on board the interferometer and can be implemented on the cubesat.

The implemented accelerometer is based upon the heritage of the ISA (Italian Spring Accelerometer) [1], developed for “BepiColombo,” the ESA cornerstone mission for the exploration of Mercury. It’s a three axis accelerometer with sensitivity equal to $10^{-10}g/\sqrt{Hz}$ in the frequency band $3.10^{-5} – 10^{-1}$Hz. Fig.1 (left) shows the mechanical implementation of one of the three accelerometer axes.

We will perform a test of a single-axis accelerometer, which has characteristics close to those necessary in an interferometric mission. In terms of signal levels, it is thought that the orbiting nanosatellite has sufficiently low noise levels, so to permit to verify the precision of the accelerometer, while we expect a rather "big" level of acceleration present in the phases of its insertion in orbit, so to verify the functionality at a high level. A more complex test is to verify the frequency response of the accelerometer. Due to the low power available in the cubesat, it is not possible to use a temperature control system; so, the accelerometer will have a spurious response in temperature that could mask the low frequencies accelerometric signal. To mitigate these effects, the accelerometer will be accompanied with a thermometer which will allow detangling thermal signals from useful signals during the post-processing analyses. The preliminary analysis of the characteristics of the cubesat indicates its suitability for this test, both for the mechanical and electrical interfacing point of view. Figure 2 (right) shows the mechanical part of the cubesat implementation of a single axis accelerometer, while in Table 2 are reported its characteristics.

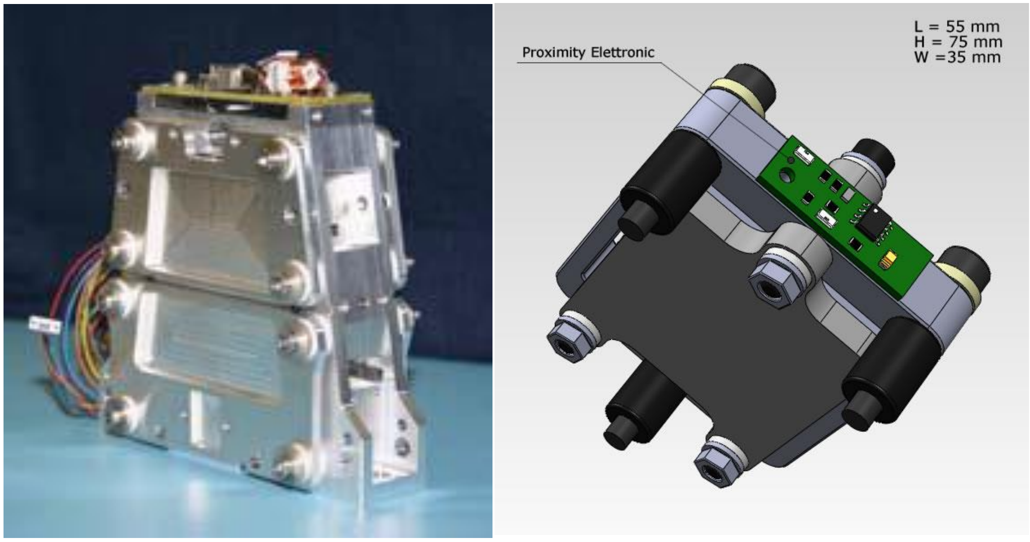

**Figure 2**: One of the 3 mechanical elements of the accelerometer

**Table 2 :** Main characteristics of the accelerometer

| | |
|---|---|
| Sensitivity($g/\sqrt{Hz}$) | 1 e-8 to 1 e-7 |
| Acquisition frequencies (Hz) | 0.1, 0.2, 0.5, 1, 5, 10, 20, 50, 100 |
| Output | Analogic or digital |
| Data rate (Bytes/s) | 250 |
| Internal thermometer precision | $< 10^{-4}$ °C |
| Communication interface | RS232 full duplex/ RS485 |
| Standard of communication | NMEA |
| Mechanical part dimensions (mm) | 80 x 60 x 25 |
| Electrical part dimension (mm) | 75 x 55 x 12 |
| Voltage supply (V) | 5 |
| Power dissipation (mW) | 75 |
| Weight (kg) | 0.2 |
| Linearity | > 80dB |
| Internal memory | SD 2Gb |

### *C. Mission purpose*

In order to generate a controlled and variable acceleration along the axis of the accelerometer, we generate, by the aid of a reaction wheel, a controlled spin around an axis perpendicular to the accelerometer axis. The accelerometer is located as far as possible from the cubesat center of mass where the rotation axis passes. A reaction wheel with 0.635 mNm maximum torque has an 11.8 mNms momentum storage capacity and a power consumption of about 0.46 watts. Consequently, the reaction wheel will be able to provide a constant angular acceleration during 18s before becoming saturated, allowing for typically one validation sequence per minute. A fully charged battery can sustain some 70 cycles. The blue curve in Figure 3 shows the variation of angular velocity (rad/s) function of time (s). The red one represents the variation of radial acceleration which can be detected by the accelerometer during one validation sequence (60s), assuming that the distance between the accelerometer and the rotation axis is 10 cm.

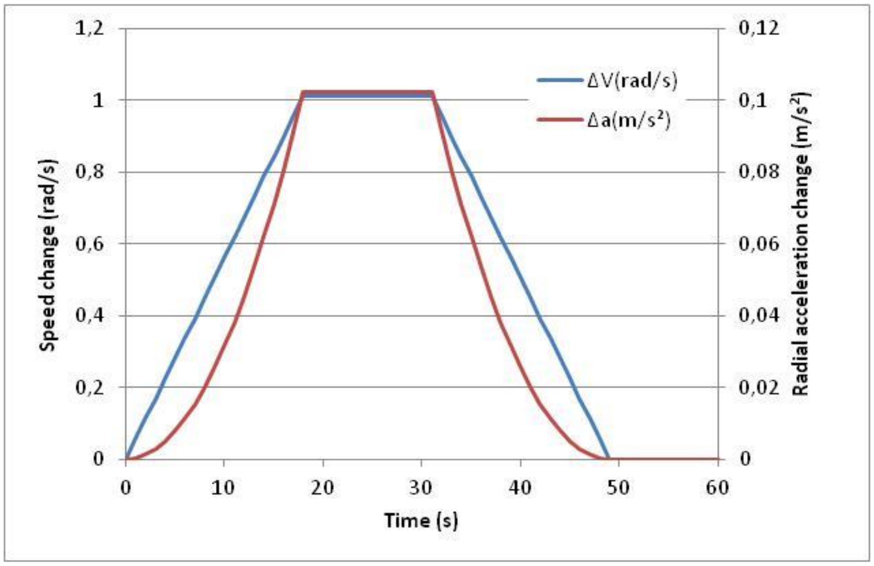

**Figure 3**: Angular velocity and radial acceleration variations.

### *D. Cubesat implementation*

Custom interfaces have been made for the accelerometer. The electronics part was split in two and set next to mechanical part in order to cut down the payload height, as shown on Figure 4. Electrical and data physical layer drivers are done by standard PC/104 pin connectors and data transfer will follow the Cubesat Space Protocol.

The main elements are:
1) supporting plates on the top and on the bottom of the accelerometer;
2) accelerometer sensor;
3) electronic pre-amplifier for the accelerometer;
4) analog electronics;
5) digital electronics.

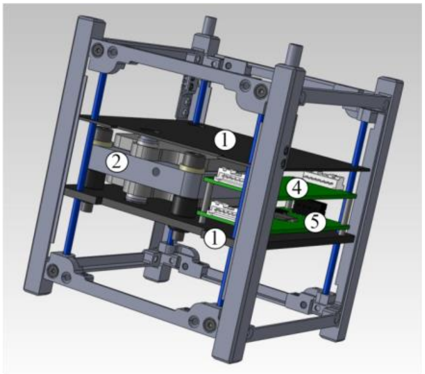

**Figure 4**: Mechanical interfaces between cubesat and accelerometer payload.

### *E. On-ground testbed*

A two-dimensional motion test-bed is considered for on-ground verification of the performance of the system. A trade-off is currently going on between two options:

- The cubesat could be set on a plate carried by a ball bearing system which will allow low-friction rotation of the setup around a vertical axis, precisely adjusted to coincide with the cubesat's centre of gravity, or
- The cubesat could be set on top of an air cushion table allowing free motion in the horizontal plane.

## V. HYPERTELESCOPE

We propose a miniature demonstrator of a kilometric multi-aperture interferometer based on the hypertelescope concept which could be flown on a nano satellite platform.

### *A. Strawman payload*

We consider a straw-man design (Figure 5) consisting of seven, meter-sized free-flying sub-apertures (D=1m) on a kilometric baseline (B=1km), organized in a non-redundant array [2]. Relying on relative movements governed by complex orbital calculations which are beyond the scope of this paper, we consider the array to be constantly re-arranging itself within this general frame, in such a way as to cover a maximum number of independent baselines within a given observing period. One option would be to force a circular movement upon the entire array, but unless the sub-apertures are linked to each other by tethers or other structures, such a movement would be extremely power consuming. Instead, quasi-linear movements, with small axial corrections and occasional course changes would probably be preferred.

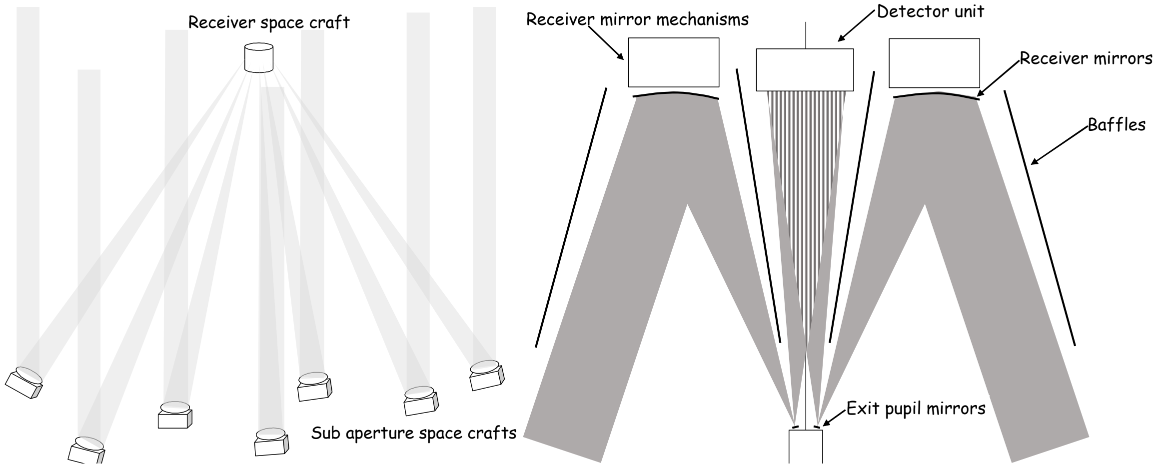

**Figure 5**: Sketch of the interferometer system (left) and the optical train of the receiver unit, fitting within a $1m^3$ box (right).

The receiver unit, ensuring interferometric recombination and detection, contains very few moving parts. Adjustments are performed by proper navigation of the SSCs (lateral movements for baseline changes, axial movements for path length adjustments, angular movements for pointing and beam transport) and tip-tilt movements of the receiver mirrors. Additional path-length adjustment could be included by adding axial movements to the receiver mirrors.

### *B. Miniaturized version to fit within a cubesat*

With the limited capacities in terms of pointing and tracking offered by CubeSat platforms, there is clearly a large amount of down-scoping required to fit such a concept. So instead of observing faint distant objects, we propose to observe the closest and brightest object at hand; the sun, and for simplicity we propose to use visible wavelengths rather than far infrared ones. With this choice, the miniaturization is imposed by the need for the object to be unresolved by the sub-apertures and barely resolved by the longest baselines. These considerations lead to apertures of 10 μm and millimetric baslines. A study of the spatio-spectral content of the solar disk compared with the optical transfer function of our interferometer is illustrated in Figure 6 [2].

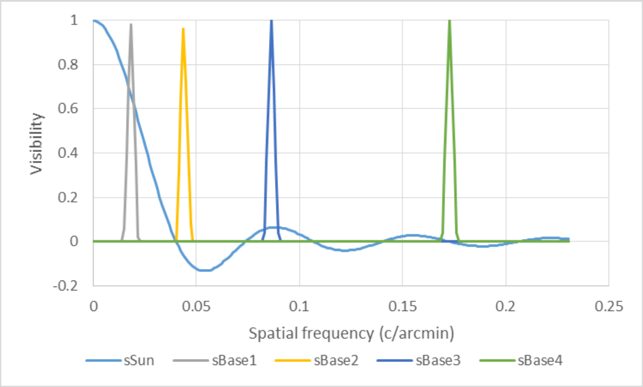

**Figure 6**: Spatial frequency analysis of interferometric imaging of the sun, assumed to be a uniform disk of diameter 30’ leading to a spatial spectrum as shown by the blue curve. The instrument modulation transfer function is shown for an interferometer working at a wavelength of 800nm with 10μm apertures and baselines of 50μm (grey), 120μm (yellow), 240μm (dark blue) and 480μm (green). This setup allows for sampling of the solar visibility function both within the high visibility inner lobe and in the low-visibility outer lobes.

### *C. Pupil layout*

For the miniature experiment we will use a fixed aperture layout, avoiding the complexity of adjustable optics. In order to simulate the gradual filling of the u-v plane, we can cover a large number of baselines by taking images at different angular orientations of the cubesat with respect to the object. Optimal design of our mask should therefore avoid duplicating baseline lengths, privileging the distribution of baseline lengths as uniformly as possible while ignoring their angular distribution. We optimized the sub aperture layout through an iterative process based on a damped least squares minimization engine (the Microsoft XL Solver) using as merit function the comparison of actual baseline lengths with a set of “ideal” lengths, corresponding to an even distribution on a linear ramp [2]. The resulting pupil layout and associated instantaneous u-v plane coverage are shown in **Figure** 7. Note that modifications of this process, allowing for example for improved angular distribution in the u-v plane, can easily be implemented by adding cost factors in the merit function.

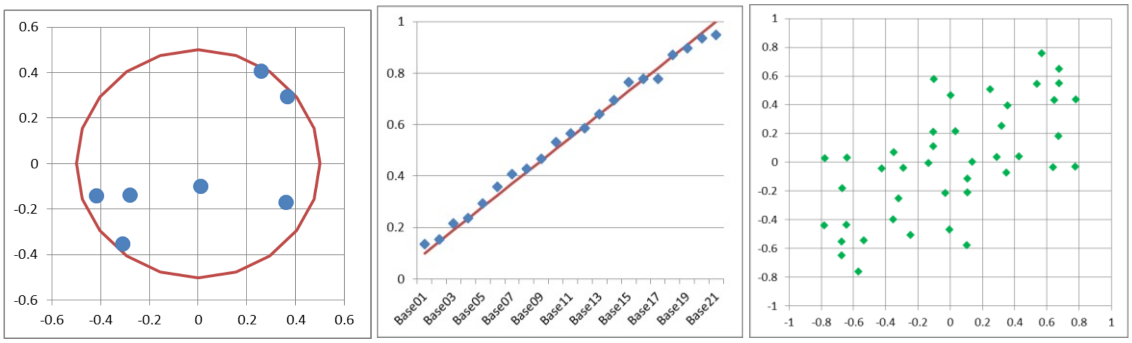

**Figure 7:** Result of the baseline optimisation process applied to the 7 sub apertures considered for our miniature experiments. Left: Pupil plane layout showing aperture positions (blue dots) in a unit diameter circle. Middle: Comparison of resulting baseline lengths (blue markers) with the ideal distribution (red line). Right: resulting instantaneous u-v plane covering. Rotating the mask between exposures allow near-perfect filling of the u-v plane with minimal redundancy.

### *D. Radiation budget*

With a solar irradiance of 1.5W/m$^2$/nm at 800nm, 5e10 photons are collected per second through a 10μm diameter aprture, leaving ample room for detection even when the light is spread over a number of detector pixels.

### *E. Navigation requirements*

Absolute pointing requirements for the cubesat-based interferometer are determined by making sure the un-resolved solar image as observed through d=10μm sub-apertures, whose angular width is λ/d = 5°, remains within the detector area. Assuming a 1k x 1k detector and a 100 pixel wide solar image, the absolute pointing therefore only needs to be within a few 10s of degrees.
Pointing stability, however, must be sufficient to avoid smearing of fringes within the exposure time. Applying the quarter-wave criterion for the longest baseline, B=0.5mm, and assuming 1s exposures, we can tolerate angular movements per second of 0.25λ/B = 1.5'.
The compatibility of these requirements with the ADCS system described above is being studied.

## VI. CONCLUSIONS

We have described the design of a cubesat platform optimized for validation of key technologies for a future far infrared interferometer mission such as FIRI. Two payloads are included, one for testing of a high-precision accelerometer, a fundamental element for the dynamic control loop of a space-based interferometer, and one allowing miniaturized demonstration of a multi-aperture interferometer in space. The proposed platform is a 2U cubesat, and we have described its design in terms of standard cubesat avionics and navigation components.

## ACKNOWLEDGEMENTS

The research leading to these results has received funding from the European Union's Seventh Framework Programme (FP7/2007-2013) under FISICA grant agreement No 312818.

## REFERENCES

[1] V. Iafolla et al, "FISICA (Far Infrared Space Interferometer Critical Assessment) Metrological problems and system requirements for interferometric observations from space", in: Metrology for Aerospace, IEEE 2014.
[2] K. Dohlen, S. Vives, E. Rakotonimbahy et al, "Design of a nano-satellite demonstrator of an infrared imaging space interferometer: the HyperCube", SPIE, June 2014 (in press).
[3] GomSpace datasheets: http://gomspace.com/index.php?p=products
[4] Maryland ASerospace datasheets: http://maiaero.com/products/mai400alacarte/